Physica B 406 (2011) 2289–2292

Contents lists available at ScienceDirect

Physica B

journal homepage: www.elsevier.com/locate/physb

Magnetic and magnetocaloric properties of perovskite manganite $Pr_{0.55}Sr_{0.45}MnO_3$

Jiyu Fan [a,*], Li Pi [b,c], Lei Zhang [b], Wei Tong [b], Langsheng Ling [b], Bo Hong [d], Yangguang Shi [a], Weichun Zhang [a], Di Lu [a], Yuheng Zhang [b,c]

[a] Department of Applied Physics, Nanjing University of Aeronautics and Astronautics, Nanjing 210016, China
[b] High Magnetic Field Laboratory, Chinese Academy of Sciences, Hefei 230031, China
[c] Hefei National Laboratory for Physical Sciences at the Microscale, University of Science and Technology of China, Hefei 230026, China
[d] Department of Material Engineering, China Jiliang University, Hangzhou 310018, China

ARTICLE INFO

Article history:
Received 30 January 2011
Received in revised form
20 March 2011
Accepted 21 March 2011
Available online 29 March 2011

Keywords:
Perovskite manganites
Magnetocaloric effect

ABSTRACT

In this paper, we have studied the magnetic and magnetocaloric properties of the perovskite manganite $Pr_{0.55}Sr_{0.45}MnO_3$. It shows a sharp paramagnetic–ferromagnetic phase transition at 291 K and possesses a moderate magnetic entropy change near room temperature. In addition, a large relative cooling power (143.64 J/kg) and a wide temperature range (84 K) have been found in this material. Compare with the Landau model, we find that the itinerant electrons mainly contribute the larger magnetic entropy change at paramagnetic region.

1. Introduction

Over the past few years, the magnetic refrigeration based on magnetocaloric effect (MCE) has attracted a great attention due to its higher energy efficiency and environmentally green technology compared to conventional gas-compression refrigeration [1]. The MCE refers to change in the temperature of the refrigerant in response to change in the external magnetic field. This effect is an intrinsic property of a magnetic material and occurs due to the change in the alignment of the magnetic moments under an applied magnetic field. As for a magnetic material, two important factors determine its large MCE. One is a large spontaneous magnetization and the other is a sharp ferromagnetic–paramagnetic (*FM–PM*) transition at Curie temperature. Earlier works showed that rare-earth metal gadolinium (Gd) was first considered as the most conspicuous magnetic refrigeration due to a large effective Bohr magnetron and high Curie temperature ($|\Delta S_m| = 10.2$ J/kg K at $\Delta H = 5.0$ T, $T_C = 294$ K) [2] However, the expensive price of Gd prevents it from the actual application. Therefore, the search for new working substance with cheap price and large MCE becomes a main research topic in this field. At present, besides some possible candidates, such as $Gd_5(Si_{1-x}Ge_x)_4$ [3], $MnAs_{1-x}Sb_x$ [4], $MnFeP_{1-x}As_x$ [5] and $Tb_{1-x}Gd_xAl_2$ [6], the hole-doped manganites with the general formula $Ln_{1-x}A_xMnO_3$ (Ln=trivalent rare earth, A=divalent alkaline earth) should be one of the most promising materials since its Curie temperature and saturation magnetization are strongly composition dependent and the magnetic refrigeration can be realized at various temperature range [7]. Furthermore, taking into account that their higher resistivity is beneficial for reducing eddy current heating, the perovskite manganites have been suggested as a strong candidate for application in magnetic refrigeration technology.

The perovskite $Pr_{1-x}Sr_xMnO_3$ is an important member in manganite family with intermediate one electron bandwidth [8]. The Pr-based manganites show many novel properties including the charge ordering (CO) state, FM and antiferromagnetic (AFM) coexistence, and metamagnetic transition [9–11]. As $x < 0.4$, it possesses a strong FM–PM phase transition and a large magnetoresistance effect. As $x \geq 0.5$, it shows a CO-antiferromagnetic (AF) state. In this paper, we select composition of $Pr_{0.55}Sr_{0.45}MnO_3$, which just lies at the boundary of FM and CO-AF phase, to investigate the MCE due to its high Curie temperature and a tunable magnetic phase boundaries which maybe possess a potential power applied in magnetic refrigeration technology.

2. Experiment

Polycrystalline $Pr_{0.55}Sr_{0.45}MnO_3$ sample was prepared by traditional solid-state reaction method [12]. The structure and phase purity of as-prepared sample were checked by powder X-ray diffraction (XRD) using Cu K_α radiation at room temperature.

* Corresponding author. Tel.: +86 25 52075729; fax: +86 25 83336919.
E-mail address: fanjiyu@gmail.com (J. Fan).

0921-4526/$ - see front matter © 2011 Elsevier B.V. All rights reserved.
doi:10.1016/j.physb.2011.03.056

The XRD patterns proved that the sample was in a single crystallographic phase, without any detectable impurity phase. The temperature dependence of magnetization was measured by a superconductive quantum interference device (SQUID) MPMS. The isothermal magnetization at selected temperatures was recorded by the SQUID-VSM system.

3. Results and discussion

Fig. 1 shows the temperature dependence of magnetization (M–T) of $Pr_{0.55}Sr_{0.45}MnO_3$ measured in the magnetic field of 100 Oe. The M–T curve exhibits a sharp PM–FM phase transition. The Curie temperature (T_C), defined by the minimum in dM/dT, has been determined to be T_C=290.8 K. In order to define T_C more exactly, the right axes of Fig. 1 present the inverse magnetization as a function of temperature. It has been fitted with the Curie–Weiss law $\chi = C/(T-\theta)$, where $C = N_A\mu_B^2 P_{eff}^2/3k_B$ is the Curie constant, N_A is Avogadro constant, μ_B is the Bohr magneton, $P_{eff} = g\sqrt{S(S+1)}$ is the effective magnetic moment, g=2 is the gyromagnetic ratio and S is the magnetic spin, k_B is Boltzmann constant, θ is paramagnetic Weiss temperature. The fitting data shows the Curie temperature is 291.2 K, in agreement with the former definition. From the fitting data of the Curie constant C, the effective magnetic moment was calculated to be $P_{eff} = 5.46\mu_B$. The inset of Fig. 1 shows the isothermal magnetization measured at 4.0 K. With the increase of the applied magnetic field, the magnetization increases sharply, and then tends to saturation as $H \geq 1.5$ T. The saturated magnetization (M_S) can be obtained from an extrapolation of the high field M–H curve to H=0, and the obtained $M_S = 3.49\mu_B$ is close to the theoretical value of $M_S = 3.35\mu_B$. According to Rhodes–Wohlfarth criterion [13], the degree of itinerancy can be determined from the ratio of P_{eff} to M_S. The ratio is close to one for the localized moment whereas it is larger than one for the itinerant moment. Here, the ratio of 1.56 for $Pr_{0.55}Sr_{0.45}MnO_3$ implies that the electrons possess an itinerant character. Since a sharp PM–FM transition occurs around 291 K, which possibly implies a large magnetic entropy change near room temperature, we performed a measurement of MCE of the present material.

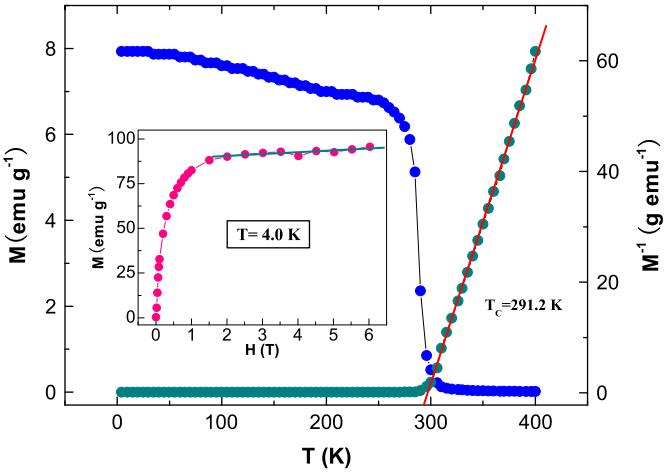

Fig. 1. Left axes: temperature dependence of magnetization measured at H=100 Oe. Right axes: the inverse of magnetization–temperature curve and the solid line is the fitting results using Curie–Weiss law. Inset: isotherm magnetization curve M–H at 4.0 K with field up to 6.0 T; the solid line is the linear fitting for the saturated magnetization.

According to the classical thermodynamical theory and Maxwell's relation, the isothermal magnetic entropy changes can be calculated as follows [14]:

$$\Delta S_M(T,H) = S_M(T,H) - S_M(T,0) = \int_0^H \left(\frac{\partial M(T,H)}{\partial T}\right)_H dH \quad (1)$$

where M is the magnetization, H is the magnetic field, and T is the temperature. In practice, the magnetic entropy change $|\Delta S_M|$ can be evaluated from the isothermal magnetization measured with small temperature intervals. For magnetization measurement performed at the small discrete field and temperatures intervals, $\Delta S_m(T,H)$ can be approximated as

$$|\Delta S_M| = \sum \frac{M_i - M_{i+1}}{T_{i+1} - T_i} \Delta H_i \quad (2)$$

where M_i and M_{i+1} are the experimental data of the magnetization at T_i and T_{i+1}, respectively, under a magnetic field H_i. In order to examine the MCE in $Pr_{0.55}Sr_{0.45}MnO_3$, as shown in Fig. 2(a), the isothermal magnetization vs applied field (M–H) was measured in different temperatures. From Eq. (1), the magnetic entropy changes depend on the value of $(\partial M/\partial T)_H$. Therefore, the large magnetic entropy changes usually occur at T_C. Using Eq. (2), the magnetic entropy change vs temperature is presented in Fig. 2(b) at various applied fields. With the increase of magnetic field, the value of magnetic entropy change increases and the peak of magnetic entropy change slightly moves to a higher temperature due to the shift of effective T_C by the applied magnetic field. At Curie temperature, the $|\Delta S_m^{max}| = 0.82$, 1.30 and 1.71 J/kg K follow by the magnetic field changes of 1.0, 2.0 and 3.0 T, respectively. Generally, from the viewpoint of active application, the relative cooling power (*RCP*) is an useful

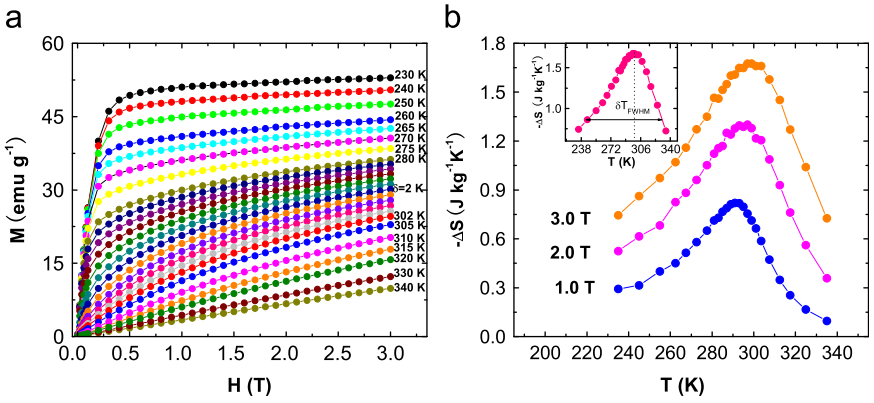

Fig. 2. (a) Isothermal magnetization vs magnetic field at different temperatures. (b) Magnetic entropy change ($-\Delta S$) plotted as a function of temperature at different applied fields; inset shows the $-\Delta S$–T curve at H=3.0 T, the line with double arrows represents the full width at half maximum of the magnetic entropy change.

parameter for selecting potential substances for magnetic refrigerants [1]. It provides a measure of how much heat can be transferred between the cold and hot sinks in an ideal refrigerant cycle. The *RCP* is defined as $RCP = -\Delta S_M^{max} \times \delta T_{FWHM}$, where ΔS_M^{max} is the maximum magnetic entropy change and δT_{FWHM} is the full width at half maximum of the magnetic entropy change curve. The material with a larger *RCP* value usually represents a better magnetocaloric material due to a high cooling efficiency. As shown in the inset of Fig. 2(b), the value of *RCP* reaches 143.64 J/kg for $\Delta H = 3$ T, which is not only commeasurable to the *RCP* of other manganites but high enough for magnetic refrigeration. Moreover, the temperature range δT_{FWHM} is found to be 84 K. This wide temperature range is very beneficial for Ericsson refrigeration cycle as well.

In order to study the origin of MCE, a simple theoretical model based on the magnetoelastic couplings and electron interaction was introduced in manganites [15,16]. Based on the Landau theory, near the Curie point of a second-order transition in the presence of an external field, the Gibbs free energy (G) can be expressed in terms of the order parameter M in the following form neglecting higher order parts:

$$G(T,M) = G_0 + \frac{1}{2}AM^2 + \frac{1}{4}BM^4 - MH \tag{3}$$

where the coefficients of A and B are temperature-dependent parameters. For the condition of equilibrium, i.e., energy minimization, $\partial G/\partial M = 0$, the magnetic equation of state is obtained as

$$H/M = A + BM^2 \tag{4}$$

Thus, the relationship of M^2 vs H/M should be shown as a linear behavior around T_C. According to the criterion proposed by Banerjee [17], the order of magnetic transition can be determined from the slope of straight line. The positive slope corresponds to the second-order transition while the negative slope corresponds to the first-order transition. Fig. 3 is an Arrott plot of M^2 vs H/M. Clearly, in the present case the positive slope of M^2 vs H/M curves indicates the phase transition is a second-order PM–FM phase transition. By differentiation of the magnetic part of the Gibbs free energy with respect to temperature, the corresponding magnetic entropy is obtained

$$S_M(T,H) = -\frac{1}{2}\frac{\partial A}{\partial T}M^2 - \frac{1}{4}\frac{\partial B}{\partial T}M^4 \tag{5}$$

In order to apply the above formulation, the temperature dependence of parameters A and B can be obtained from the linear fitting of the Arrott plot of H/M vs M^2 by using Eq. (4). The parameters A and B correspond to the intercept on H/M axis and the slope of the liner fitting, respectively. As shown in the inset of Fig. 3, one can find that the parameter A varies from negative to positive values with increasing temperature, and the temperature just corresponding to the zero value of parameter A is consistent with the T_C. The elastic and the magnetoelastic terms of free energy are included in parameter B, and the parameter is positive for a ferromagnet with the second-order phase transition [18]. Using parameters A and B extracted from the data, the temperature dependence of magnetic entropy $S(T,H)$ under the variational magnetic field can be calculated. Nevertheless, in order to compare with the magnetic entropy change ($\Delta S(T,H)$) obtained for experimental measurements, we should also calculate the temperature dependence of magnetic entropy without magnetic field $S(T,H=0)$. Therefore, the theoretical magnetic entropy change $\Delta S_L(T,H)$ is

$$\Delta S_L(T,H) = S_M(T,0) - S_M(T,H) = -\frac{1}{2}\frac{\partial A}{\partial T}(M_0^2 - M^2) - \frac{1}{4}\frac{\partial B}{\partial T}(M_0^4 - M^4) \tag{6}$$

Here, the value of M_0 can be obtained by extrapolating the magnetization at $H=0$. As shown in Fig. 4, the open circle represents the calculated magnetic entropy change by using Eq. (6). Obviously, the experimental curves and theoretical curves are roughly appropriate. However, two important distinctive features are worthy of our attention. The first one is the temperature of ΔS_M^{max} in the theoretical curves lower than that in the experimental curves. As for the theoretical curves, the temperature of ΔS_M^{max} remains unchange irrespectively of magnetic field variation whereas the temperature moves to the higher region with magnetic field in the experimental curves. As mentioned in the previous discussion, the temperature of ΔS_M^{max} can be driven by the magnetic field to the higher region. The second one is that the experimental curve is consistent with the calculated curve in the FM region, whereas an obvious deviation between them occurs in the PM region. Moreover, the calculated values are smaller than that from the experimental values. Recently, Koubaa et al. reported the ΔS_M values in $La_{0.8}K_{0.1}M_{0.1}MnO_3$ (M=Na/Ag) determined by Maxwell theory agree well with that calculated by the above Landau theory [19]. They proposed that magnetoelastic coupling and electron interaction contributed to magnetic entropy change. However, both of two samples are at optimal doping region ($x=0.3$) while our sample is near to half-doping

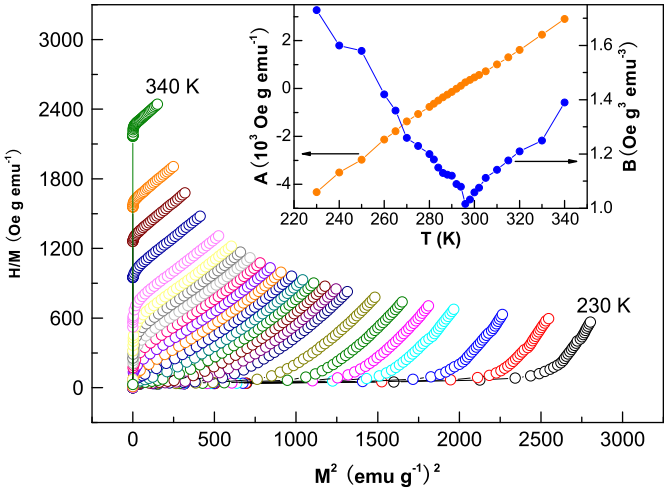

Fig. 3. Arrott plot: isotherms of H/M vs M^2 at different temperatures close to the Curie temperature (T_C=291 K). The inset shows temperature dependence of parameters A (left hand) and B (right hand).

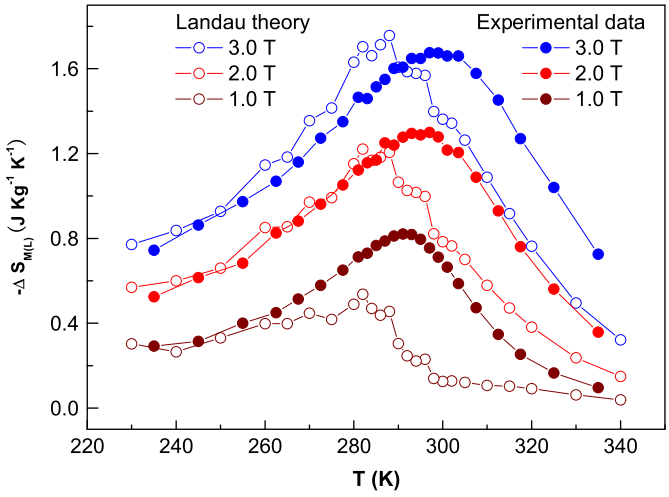

Fig. 4. The calculated and experimental values of magnetic entropy change as a function of temperature under field change $\Delta H = 1.0$, 2.0 and 3.0 T, respectively.

region ($x=0.5$). Therefore, in order to clarify the reason, let us now return to the initial discussion about the calculation of MCE from isothermal M–H curves. The experimental curves of magnetic entropy change were obtained from Maxwell's relation, where the entropy change should be referred to be a total entropy change, namely, ΔS_M includes three contributions:

$$\Delta S_M(T,H) = \Delta S_1(M) + \Delta S_2(E) + \Delta S_3(C) \quad (7)$$

where $\Delta S_1(M)$ is the net magnetic entropy change, $\Delta S_2(E)$ is the entropy change of electron, and $\Delta S_3(C)$ is the entropy change of crystal lattice. Since the isotherms magnetization was measured in the present investigation, the contribution of crystal lattice $\Delta S_3(C)$ can be ignored. Therefore, the experimental curves involve two parts of $\Delta S_1(M)$ and $\Delta S_2(E)$. However, as for the theoretical curves, they were obtained from the Gibbs free energy, where it only considers the contribution of magnetic field rather than involve the entropy change of electron. Thus, the theoretical entropy change only describes the first part of Eq. (7), namely, $\Delta S_L = \Delta S_1(M)$. Therefore, the entropy change of electron is the main reason for the obvious deviation in Fig. 4. As $T > T_C$, the itinerant electrons are in disorder state and they will produce a large entropy change when the magnetic field is applied. On the contrary, as $T < T_C$, the system has undergone a PM–FM phase transition. The itinerant electrons themselves automatically form an order structure due to the inner FM interaction and a strong on-site Hund's rule coupling. Hence, the electronic entropy change is very small even under a large applied magnetic field. Therefore, the theoretical curves almost superpose the experimental curves at FM region. In fact, as for manganites which PM–FM phase transition is accompanied by the metal–insulator transition, Kamilov et al. ever pointed out that the electronic entropy caused some small deviations from accurate MCE [20]. In addition, the indirect measurement is also a possible reason for the discrepancies.

4. Conclusion

In summary, we have studied magnetocaloric effect near room temperature and FM interaction of $Pr_{0.55}Sr_{0.45}MnO_3$. The experimental results indicate that the present material possesses a large RCP and a wide temperature range δT_{FWHM}. Compare with the theoretical calculation with Landau model, the obtained larger magnetic entropy change at paramagnetic region stems from the contribution of the itinerant electrons.

Acknowledgments

This work was supported by NUAA Research Funding (Nos. NS2010187 and NS2010208) and Astronautics and the National Nature Science Foundation of China (Nos. 10904149, 11004196, 11004194, 10334090, and 51001061).

References

[1] K.A. Gschneidner Jr., V.K. Pecharsky, A.O. Tsokol, Rep. Prog. Phys. 68 (2005) 1479.
[2] S.Yu. Dankov, A.M. Tishin, V.K. Pecharsky, K.A. Gschneidner Jr., Phys. Rev. B 57 (1998) 3478.
[3] V.K. Pecharsky, K.A. Gschneidner, Phys. Rev. Lett. 78 (1997) 4494.
[4] H. Wada, Y. Tanabe, Appl. Phys. Lett. 79 (2001) 3302.
[5] Q. Tegus, E. Bruck, K.H. Buschow, F.R. de Boer, Nature 415 (2002) 150.
[6] F.W. Wang, X.X. Zhang, F.X. Hu, Appl. Phys. Lett. 77 (2000) 1360.
[7] M.-H. Phan, S.-C. Yu, J. Magn. Magn. Mater. 308 (2007) 325.
[8] E. Pollert, Z. Jirák, J. Hejtmánek, A. Strejc, R. Kužel, V. Hardy, J. Magn. Magn. Mater. 246 (2002) 290.
[9] T. Wu, M. Mitchell, Phys. Rev. B 69 (2004) 100405(R).
[10] S. Hebert, A. Maignan, V. Hardy, C. Martin, M. Hervieu, B. Raveau, R. Mahendiran, P. Schiffer, Eur. Phys. J. B 29 (2002) 419.
[11] R. Mahandiran, A. Maignan, S. Hebert, C. Martin, M. Hervieu, B. Raveau, J.F. Mitchell, P. Schiffer, Phys. Rev. Lett. 89 (2002) 286602.
[12] J. Fan, L. Ling, B. Hong, L. Pi, Y. Zhang, J. Magn. Magn. Mater. 321 (2009) 2838.
[13] J. Kubler, Theory of Itinerant Electron Magnetism, Clarendon Press, Oxford, 2000.
[14] V.K. Pecharsky, K.A. Gscheidner, J. Magn. Magn. Mater. 200 (1999) 44.
[15] V.A. Amaral, J.S. Amaral, J. Magn. Magn. Mater. 272 (2004) 2104.
[16] J.S. Amaral, M.S. Reis, V.A. Amaral, T.M. Mendonca, J.P. Araúji, M.A. Sá, P.B. Tvares, J.M. Vieira, J. Magn. Magn. Mater. 290 (2005) 686.
[17] S.K. Banerjee, Phys. Lett. 12 (1964) 16.
[18] L.D. Landau, E.M. Lifshitz, Statistical Physics, third ed., Pergamon, Oxford, 1980.
[19] M. Koubaa, Y. Regaieg, W. Cheikhrouhou Koubaa, A. Cheikhrouhou, S. Ammar-Merah, F. Herbst, J. Magn. Magn. Mater. 323 (2011) 252.
[20] I.K. Kamilov, A.G. Gamzatov, A.M. Aliev, A.B. Batdalov, A.A. Aliverdiev, Sh.B. Abdulvagidov, O.V. Melnikov, O.Yu. Gorbenko, A.R. Kaul, J. Phys. D Appl. Phys. 40 (2007) 4413.